Journal of Hydrology 573 (2019) 207–219

Contents lists available at ScienceDirect

Journal of Hydrology

journal homepage: www.elsevier.com/locate/jhydrol

Research papers

A decision-making model for flood warning system based on ensemble forecasts

Leila Goodarzi, Mohammad Ebrahim Banihabib*, Abbas Roozbahani

Dept. of Irrigation and Drainage, College of Aburaihan, University of Tehran, Iran

ARTICLE INFO

This manuscript was handled by Emmanouil Anagnostou, Editor-in-Chief, with the assistance of Efthymios Nikolopoulos, Associate Editor

Keywords:
Bayesian networks
Ensemble flood forecasting
Flood warning
Fuzzy-TOPSIS
WRF model

ABSTRACT

The purpose of this study is to develop a flood warning system based on Atmospheric Ensemble Forecasts. Although ensemble forecasts are increasingly employed for flood forecasting, developing a flood warning system based on ensemble forecasts has not been adequately addressed yet. In this study, first a Weather Research and Forecasting (WRF) model was used to forecast the heavy precipitation in Kan Basin, Iran. Ensemble storms were forecasted using five cumulus schemes including Kain-Fritsch, Betts-Miller-Janjic, Grell 3D ensemble, Multi-scale Kain-Fritsch and Grell-Devenyi ensemble cumulus scheme. Then, a Bayesian Networks (BN) was developed to estimate the flood peak using the atmospheric ensemble forecasts. Finally, a Fuzzy-TOPSIS (The Technique for Order of Preference by Similarity to Ideal Solution) model was prepared for making decisions for flood warning scenarios considering all effective factors in flood warning and uncertainty associated with them. Assessment of the proposed flood warning system was examined for various scenarios. It showed that when a significantly high probability was assigned to a warning level, that level had the maximum closeness coefficient and consequently chosen as a warning level. Yet, if the probability was distributed equally between some warning levels, the flood warning system acts cautiously since the decision-making model allocated the highest rank to the stronger warning level. Regarding the reasonable results of this study, applying the Fuzzy-TOPSIS model to develop a flood warning system based on atmospheric ensemble forecasts is recommended to apply in similar catchments for addressing the uncertainties.

1. Introduction

Quantifying the uncertainties of flood forecasting is becoming increasingly essential for operational purposes (Komma et al., 2007). Furthermore, as atmospheric forecasts are used for flood forecasting, their uncertainties should be considered in the flood forecasting (Dietrich et al., 2009b). In order to address these uncertainties, many operational flood forecasting systems are increasingly moving towards the application of ensemble flood forecasts rather than single deterministic forecasts (Cloke and Pappenberger, 2009). Various approaches have been presented to forecast atmospheric ensemble forecasts including perturbing the input parameters of the model, perturbing the initial conditions, using multi-model ensembles and using different parameterization schemes (Yang et al., 2012).

Numerical Weather Prediction (NWP) models are used for atmospheric forecasting. The spatial resolution of NWP models is sometimes too coarse to consider the physical processes including momentum, heat, and humidity turbulence fluxes and thus these phenomena have to be parameterized in these models (Shrivastava et al., 2014). Generate an ensemble (or set) of different forecasts of atmospheric processes, differed by using various parameterization schemes, is the standard method of addressing the parameterization uncertainty. One of the most important parameterization schemes in rainfall forecasting is the cumulus parameterization (Nasrollahi et al., 2012). NWP models often use Cumulus Parameterization Schemes (CPS) to address the effects of cumulus clouds which are not represented in the modelling as they are much smaller than the model grid size (Pennelly et al., 2014).

The Weather Research and Forecasting (WRF) model has been widely applied for atmospheric research and operational forecasting. The WRF model has different physical parameterization schemes including CPS (Nasrollahi et al., 2012). Common CPS are: Kain-Fritsch (KF) (Kain and Fritsch, 1990), Betts-Miller-Janjic (BMJ) (Janjić, 1994), Grell 3D ensemble (GR3D) (Grell, 1993), Multi-scale Kain-Fritsch (MSKF) (Zheng et al., 2016) and Grell-Devenyi ensemble (GDE) (Grell and Dévényi, 2002). Each Cumulus parameterization has its unique structure and complexity, which may have a great effect on the precipitation simulations. Accordingly, various sensitivity analyses of the WRF parameterizations have been carried out in different areas of the

* Corresponding author.
E-mail addresses: Goodarzi.1988@ut.ac.ir (L. Goodarzi), banihabib@ut.ac.ir (M.E. Banihabib), Roozbahany@ut.ac.ir (A. Roozbahani).

https://doi.org/10.1016/j.jhydrol.2019.03.040
Received 24 October 2018; Received in revised form 24 February 2019; Accepted 3 March 2019
Available online 16 March 2019

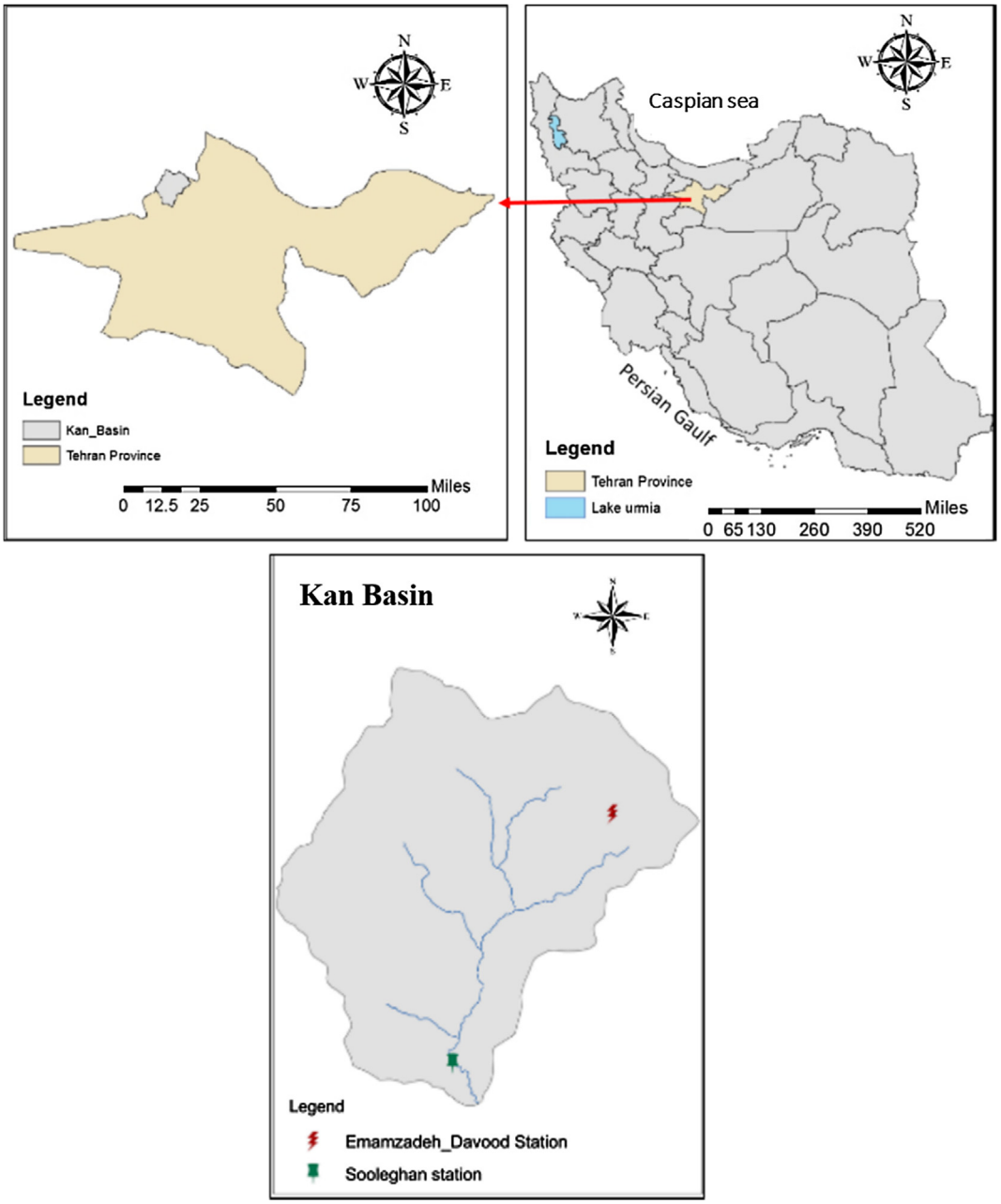

Fig. 1. Location of study area.

world (Klein et al., 2015). Guoqiang et al. (2007) compared the continuous precipitation process forecasted with the results obtained by the WRF model. The comparison results displayed that the KF scheme was better than the BM (Betts-Miller) scheme in summer time. Pennelly et al. (2014) employed the WRF model to simulate precipitation in Alberta, Canada. The results reveal that the Kain–Fritsch and explicit cumulus parameterization schemes were the most accurate schemes. Application of the WRF model to simulate six storm events in China, by Tian et al. (2017), showed that the BMJ scheme was unsuitable for rainfall simulation in their study area. Therefore, the accuracy of NWP models' results can be quite dependent on the cumulus parameterization used in the study.

Ensemble meteorological forecasting is widely combined with a hydrological model to forecast flood events. Li et al. (2017) combined the WRF model with a hydrological model for ensemble flood forecasting in China. According to obtained results, the simulated floods were rational and could benefit the flood management because of its longer lead time. Rogelis and Werner (2018) evaluated the potential of NWP models for flood warning in tropical mountainous watersheds. The results showed that the flow forecasts by a hydrological model added value to the flood early warning systems. Although ensemble forecasts are increasingly employing in flood forecasting around the world, developing a flood warning system based on ensemble forecasts has not adequately addressed yet. For instance, limited studies reported how flood hydrographs can be converted into warning decisions during a flood event (e.g. using of threshold exceedance). Abebe and Price (2005) developed a decision support system for a flood early warning in two urban areas in Italy and Greece. They proposed several flood threshold levels and estimated the magnitude and the probability of flood employing the number of exceeding ensemble members for each flood threshold. Dietrich et al. (2009b) used a subset of the super-ensemble and the quantile of the forecasted flow ensemble, which was a good predictor for particular warning levels. Yang et al. (2016) developed an early flood warning system in Taiwan applying integrating

ensemble rainfall forecasts, rainfall thresholds, and a real-time data assimilation process to evaluate the possibility of flood alerts. Other conceptions of deriving a single (i.e. deterministic type) warning indicator from ensemble forecasts are weighting ensemble members including Bayesian Model Averaging (BMA) by Raftery et al. (2005), getting machine learning by Doycheva et al. (2016), and decreasing ensemble members to produce a multi-model super-or sub-ensemble (Dietrich et al. (2009a)). In the mentioned studies, only a few effective criteria such as the probability of flood occurrence and vulnerability of the area were considered for flood warning decision making and other effective criteria including flood warning costs, flood economic damages, the population at risk and expected cost of false warnings were ignored in flood warning decisions. Likewise, the uncertainty of different criteria has been ignored in the decision making of flood warning. The present research tries to provide a flood warning system addressing all effective criteria and uncertainty associated with them, since the false warnings may cause distrust of the inhabitants. One of the main problems in ensemble flood warning is estimation of the flood peak discharge magnitude and the probability of flood occurrence for an ensemble of hydrographs with a large spread of forecasted flood peaks. In accordance to this problem, Bayesian Network (BN) was employed in this study to estimate the flood peak magnitude in an ensemble forecasting. Moreover, a Fuzzy-TOPSIS (The Technique for Order of Preference by Similarity to Ideal Solution) model has been used to incorporate different criteria in flood warning decision making.

2. Methodology

2.1. Study area

The present study was conducted for the Kan Basin, Tehran, Iran. Over the past several decades, heavy rainfalls have caused flood events and huge damage in this basin. The catchment area is 197 km^2 located between 35°46′ N to 35°58′ N latitudes and 51°10′ E to 51°23′ E longitudes. The average annual precipitation is 600 mm and the average slope of the basin is approximately 42.4%. In the present study, the assessment of heavy rainfall was carried out on the Emamzadeh-Davood rainfall station. Moreover, the flood assessment was performed on Sulaghan hydrometric station, located downstream of the study area shown in Fig. 1. The present study was conducted on 14 historical storms. The data sample set is relatively small in this study due to the following reasons:

1) NCEP (GFS - FNL) data are available from 2000 onwards on the website.
2) During the above-mentioned period, there are small numbers of observed flood events in the study area because of the location of the Kan River basin in semi-arid regions and experienced long drought period with fewer flood events.

Fig. 2 shows the main steps of the proposed flood warning system in the present study. According to this flowchart, the heavy rainfalls are forecasted using the WRF model, peak flood is forecasted using a BN model and a flood warning system is developed using the Fuzzy-TOPSIS model.

2.2. WRF model

The WRF model is a next generation's medium-range weather and research forecasting model that can simulate weather processes from cloud scale to synoptic scale. All precipitation simulations in this study were conducted with the Advanced Research WRF (WRF-ARW) version 3.8. The initial and lateral boundary conditions are extracted from National Centers for Environmental Prediction (NCEP), Global Forecast System (GFS). The data are 6-hourly global analysis at 0.5∘ horizontal resolution. The Noah land surface model (Chen and Dudhia, 2001), as well as the Yonsei University (YSU) planetary boundary layer scheme (Hong et al., 2006), were used as the physic schemes. Other applied physics schemes are Rapid Radiative Transfer Model (RRTM), longwave radiation scheme (Mlawer et al., 1997), the Dudhia shortwave radiation model (Dudhia, 1989) and the WRF Single-Moment (WSM) 3-class microphysics scheme (Hong et al., 2004). Because of the importance of cumulus parameterization in rainfall and hydrological analysis, a meteorological ensemble was created by using five cumulus schemes including Betts-Miller-Janjic (BMJ), Kain-Fritsch (KF), Grell 3D ensemble (GR3D), Multi-scale Kain-Fritsch (MSKF) and Grell-Devenyi ensemble (GDE). Figure 3 illustrates the domains setup using an inter-active nested domain inside the parent domain. The temporal resolution of WRF is 1 h and horizontal resolution of nested domains are 45 km, 15 km, and 5 km, respectively. The inner domain covers the study basin, and only the meteorological information from this domain was used in the present study. Since increasing of lead time leads to decreasing the accuracy of numerical weather model (Sikder and Hossain, 2016), all precipitation forecasts were conducted one day before the event. The nearest-neighbor interpolation was used to assign a predicted rainfall value to the rain gage.

2.3. Bayesian network

A Bayesian network (BN) was employed in this study to forecast the peak flood based on the meteorological ensemble forecasts. A BN model is a probabilistic graphical model that consists of a set of variables (nodes) and their probabilistic conditional independencies (encoded in its arrows) (Correa et al., 2009). A node represents a random variable and an arrow shows dependency/independency of a node on other nodes. The arrow starts from a casual or predictor event of the parent node and connects to an outcome event of the child node or predicting node. The relationship between various nodes is defined in a conditional probability based on prior information (or data) and statistically observed correlations (Sharma and Goyal, 2016). A graph containing nodes and arrows is called BN structure (BS). There are many possible structures for a set of data. The purpose of structure learning is to determine the best structure, which maximizes the conditional probability P(BS|D), where BS is the BN structure and D is the given data (Sharma and Goyal, 2016). Some common structure learning algorithms are the K2 algorithm (Cooper and Herskovits, 1992) and MCMC algorithm (Madigan et al., 1995). In the present study, the relationships between child and parent nodes are known, so BS can be easily defined. The flood peak is a child node that is influenced by some parent nodes including atmospheric ensemble forecasts, the base flow of the river and antecedent rainfall, so the BS is known. The catchment's antecedent moisture represents the relative wetness prior to a flood event and it can have a significant influence on overall flood response. Because of the lack of antecedent moisture data in the study area, antecedent rainfall was used instead of it.

Ten different scenarios presented in Table 8 were developed using different combinations of predictors. Once the structure was defined, it was necessary to know how strong the relationship is among the variables that were realized by using the quantitative component of the BN (Aguilera et al., 2011). The joint probability (P_b) among the variables can be defined as the product of the local conditional distributions, so that:

$$P_b = (x_1, x_2, \ldots, x_n) = \prod_{i=1}^{n} P_b(x_i | x_{i+1}, \ldots, x_n) \quad (1)$$

In a BN, a node x_i is independent of all other nodes except its parents (πi) (Sharma and Goyal, 2016). A simple example of BN is presented in Fig. 4. The joint probability for this simple network can be defined as Eq. (2):

$$p(x_1. x_2. x_3) = p(x_1) \times p(x_2|x_1) \times p(x_3 | x_1. x_2) \quad (2)$$

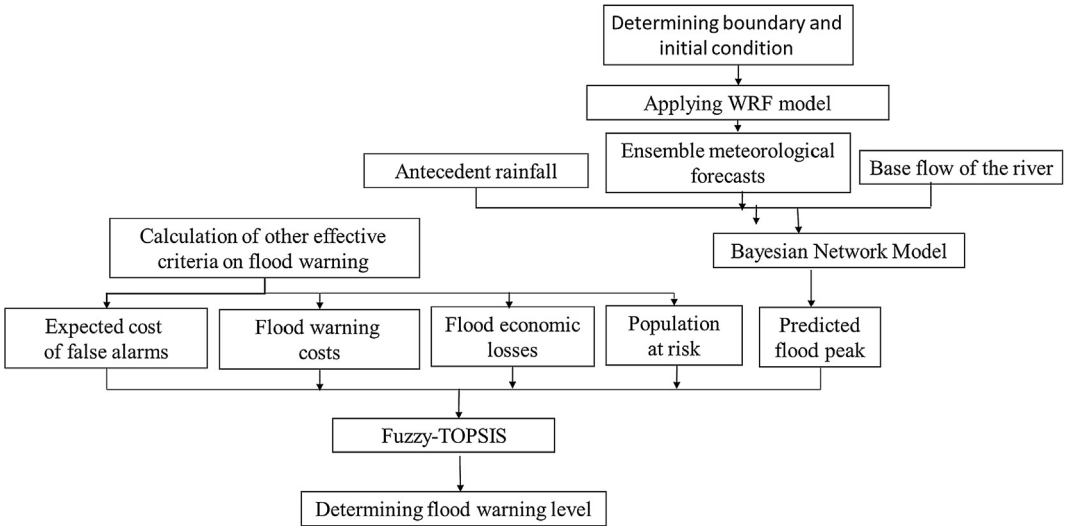

Fig. 2. Flowchart of main steps for flood warning system in the present study.

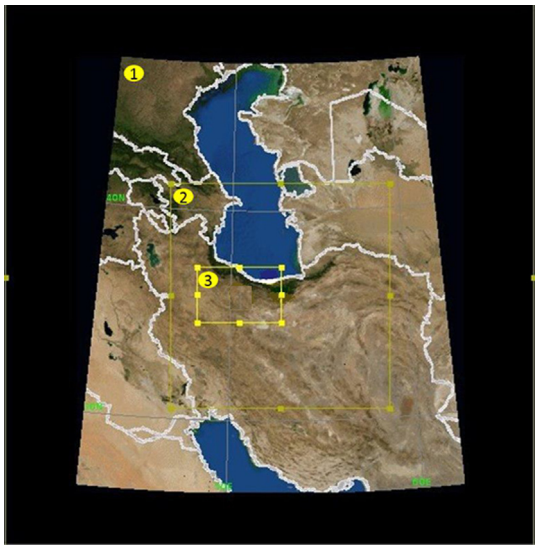

Fig. 3. WRF domain setup using an inter-active nested domain inside the parent domain.

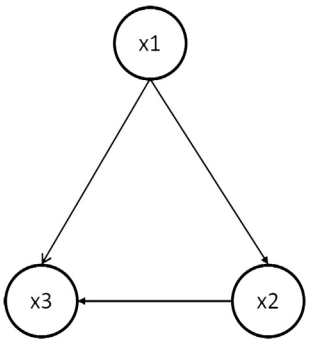

Fig. 4. An example of graphical Bayesian network.

Bayesian network conditional probability tables (CPTs) can be learned (trained) by using parameter learning algorithms including Expectation Maximization, Markov Chain Monte Carlo methods such as Gibbs sampling, and gradient descent methods (Reed and Mengshoel, 2014). In the present study, Expectation Maximization (EM) was applied for Bayesian Network parameter learning that is an iterative method that performs a number of iterations, each of which calculates the logarithm of the probability of the data given the current joint probability distribution. This quantity is known as the log-likelihood, and the algorithm tries to maximize likelihood estimators (Bergmann and Kopp, 2009). The HUGIN software (version 8.3) were used to develop the probabilistic Bayesian network structure. Final step is the validation in which the accuracy of the trained BN model is evaluated using assessment criteria. In the present study, mean absolute relative error (*MARE*) was used for performance assessment of the model as given in the following equation:

$$MARE = \frac{1}{n}\sum \frac{|O_i - F_i|}{O_i} \quad (3)$$

where, O_i is the observed value, F_i is forecasted value and n is the total number of data sets.

It should be noted that 70% of the available data is allocated for training and the remaining (30%) data are used for validation. Considering the relatively small sample size in the study area, we proposed using the Bayesian network that is less sensitive to small data set size in comparison with other forecasting models (Zhang and Bivens, 2007).

2.4. Flood warning system

An effective flood warning system should be based on all effective factors in flood warning and uncertainty associated with them. In this study, a Multi-Criteria Decision Making (MCDM) model was applied to determine the flood warning level. We proposed a FUZZY-TOPSIS model to develop a flood warning system based on ensemble forecasts that were employed to find the best flood warning level among different alternatives using various decision criteria including probability of flood occurrence, flood warning costs, flood economic damages, population at risk, expected cost of false warning and expected human losses of missed warnings under uncertainty condition. Four warning levels were considered as the decision alternatives as defined in Table 1.

Table 1
Definition of different warning levels in this study.

Flood warning level	Definition
Low	a 25-year return period flood
Medium	a 100-year return period flood
High	a 200-year return period flood
Extreme	greater than a 200-year return period flood

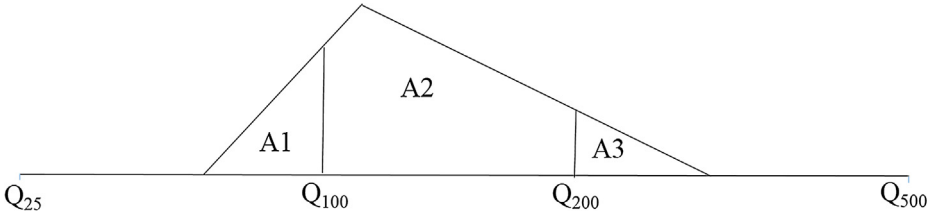

Fig. 5. Triangular membership for the forecasted flood peak.

2.5. Effective criteria in decision making

2.5.1. Probability of flood occurrence

As discussed earlier in Section 2.3, the flood peaks were forecasted using the most accurate scenario of the BN model. It should be noted that the forecasted flood peak by each scenario is a crisp value. To address the uncertainty in forecasting of flood peaks, the forecasted flood peak by the most accurate scenario was considered as the middle value of the fuzzy number and the upper and lower bounds of fuzzy numbers were determined according to the minimum and maximum forecasted flood peaks among the output of different scenarios of using BN models. A membership value is assigned to the members using the triangular membership function. For this purpose, *a membership value of one was assigned to the middle value of fuzzy number and zero was assigned to* the upper and lower bounds fuzzy numbers. An example of a hypothetical flood peak and the triangular membership is presented in Fig. 5. Q25 shows the 25-year flood which is representative for Low warning level. The other warning levels have been also showed similarly in the Figure. The probability of a warning level was estimated by dividing the area enclosed by upper and lower bounds of that level by the total area under the fuzzy triangle. It should be noted probability of a warning level was estimated as a crisp number. For example, the probability of the high warning level was calculated using the following equation:

$$P(Q_{100-200}) = \frac{A_2}{A_1 + A_2 + A_3} \tag{4}$$

2.5.2. Populations at risk

The integration of land use and flood mapping was used to identify the population at risk in a flooded area. The population at risk was calculated by multiplying the flooded area by population density in the study area. According to the field investigation of the study area, the buildings are mostly one to three floors, so the population density corresponding to one and three-floor buildings was respectively used to get upper and lower uncertainty bounds of the population at risk.

2.5.3. Flood warning costs

Warning cost includes transporting the people under flood risk to a safe place, temporary re-locating of them for two days. Since the uncertainty of transporting and the food is negligible, only the uncertainty of temporary re-locating was addressed here.

2.5.4. Flood economic damages

It includes damages to buildings and orchards in flood zones. The overlaying of land use map and flood zoning map was used to identify the buildings at risk in flood zones. Percentage of buildings damage was calculated using the depth-damage functions as shown in Table 2. Flood damage on buildings was calculated using the following equation:

Table 2
Percent damage for residential structures in flooded area.

Flood depth *(m)*	< 0.2	0.2–0.5	0.5–1	1–1.5	> 1.5
Percent damage	5	15	25	40	50

$$L_b = A \times P \times D \tag{5}$$

That L_b is flood damage on buildings, A is the area of buildings at risk (m^2), P is the house building price per square meter (Iranian Rial/m^2) and D is a percentage of building damage.

Since the building materials are different, the upper and lower bounds of price were estimated according to the civil engineering experts' judgments. The construction price of each square meter of the building was considered ten million Iranian Rials (IRR) with 20% uncertainty.

In order to calculate the flood damage to orchards, the overlaying of land use map and flood zoning map was used to identify the flood damages on orchards. Percentage and yield of different type of orchards in the study area are presented in Table 3. The percentage of damage to agricultural products depends on the depth and duration of submergence. According to Table 4, damage percentage of orchards was estimated. Finally, the damage to orchards was calculated using the following equation:

$$L_O = \sum_{i=1}^{n} (A_i \times R_i \times P_i \times D_i \times 1000) \tag{6}$$

That A_i is the area of orchards (hectare), R_i is the yield of products (ton per hectare), P_i is the price of one kilogram of products (IRR), D_i is percentage of damage and i refers to different type of orchards.

2.5.5. Expected cost of corrupted warnings

Corrupted warning includes two kind of warning: false warning and missed warning. False warning mean forecast shows the occurrence of the flood but it does not occur. False warnings can cause extra costs to notify and relocate residents. On the other hand, missed warnings (missing warning of occurred floods) can cause economic damages. In the case of missed warnings, economic damages arise in the unwarned flooded area. In this case study, personal property of residents was estimated between 10 and 30 million IRR for each resident. Expected cost formula for different warning levels presented in Table 5. That C_i is warning costs of i^{th} warning level, D_i is economic damages, f_i is the probability occurrence of i^{th} warning level.

For instance, expected cost formula for Medium warning level in Table 5 is described as following. If a medium flood with f_2 probability is announced, f_1, $f_3 and f_4$ are probability of Low, High and Extreme warning levels. Therefore, three different status of corrupted warnings may occur as following:

Component 1: An extreme flood leads to economic damages equal to the area between protected personal property in medium level and extreme level($D_4 - D_2$). Since the probability of the extreme level is equal to f_4, the expected damages of this component is equal to

Table 3
Percentage and yield of different type of orchards in the study area.

Types of orchards	Percentage of orchards in the study area	Yield (tons per hectare)
Peach	12.5	23
Cherry	66.7	14
Apple	14.6	18
Blackberry	2.1	2
Walnut	4.2	3

Table 4
Percent damage for orchards in the flooded area.

Duration of submergence > 24 h			Duration of submergence < 24 h	
Flood depth (m)	> 0.6	≤0.6	> 0.6	≤0.6
Percentage of damage	100	75	88	54

Table 5
Expected cost of corrupted warning.

Warning Level	Expected cost formula
Low warning (level 1)	$f_4(D_4 - D_1) + f_3(D_3 - D_1) + f_2(D_2 - D_1)$
Medium warning *(level 2)*	$f_4(D_4 - D_2) + f_1(C_2 - C_1) + f_3(D_3 - D_2)$
High warning *(level 3)*	$f_2(C_3 - C_2) + f_4(D_4 - D_3) + f_1(C_3 - C_1)$
Extreme warning *(level 4)*	$f_3(C_4 - C_3) + f_2(C_4 - C_2) + f_1(C_4 - C_1)$

$f_4 \times (D_4 - D_2)$.

Component 2: A high flood leads to economic damages equal to the area between protected personal property in medium level and high level$(D_3 - D_2)$. Since the probability of the high level is equal to f_3, the expected damages of this component is equal to $f_3 \times (D_3 - D_2)$.

Component 3: A low flood leads to extra costs equal to the area between warning costs in medium and low levels$(C_2 - C_1)$. Since the probability of the low level is equal to f_1, the expected extra costs is equal to $f_1 \times (C_2 - C_1)$.

Finally, the total expected costs are achieved by integration of the three components.

2.5.6. The expected human losses of missed warnings

For the cases of missed warnings, expected human losses were calculated using the populations at risk living in between flooded area of forecasted warning level and occurred flood as shown in Table 6. Where P_i is populations at risk in i*th* warning level and f_i is the probability occurrence of i*th* warning level.

2.6. Fuzzy-TOPSIS for flood decision making

Since the effective criteria in flood warning can have different importance for decision making, a Fuzzy-TOPSIS model was employed to develop a flood warning decision model considering all effective factors in flood warning and uncertainties associated with it. Pairwise comparisons matrix was defined by the expert committee and the criteria weight vector was calculated using the Saaty's method. The Fuzzy-TOPSIS model was proposed for ranking the warning alternatives. Fuzzy-TOPSIS model adapted from Wang and Chang (2007) as the following steps:

Step 1: In order to avoid the arbitrary selection of the weights, the matrix was constructed using the consensus of the expert committee with the scale of integers between 1 and 9. Among all expert's values, the minimum, maximum and average of all expert's values were considered as the lower band, upper band and the middle of the fuzzy triangular numbers.

Step 2: The weighting of effective criteria was determined using Saaty's method. The readers are referred to the Saaty (1987).

$$W = [w_1.\ w_2.\ \cdots.w_n] \tag{7}$$

Table 6
Expected human losses of missed warnings.

Warning Level	Expected human losses
Low warning (level 1)	$f_4(p_4 - p_1) + f_3(p_3 - p_1) + f_2(p_2 - p_1)$
Medium warning *(level 2)*	$f_4(p_4 - p_2) + f_3(p_3 - p_2)$
High warning *(level 3)*	$f_4(p_4 - p_3)$
Extreme warning *(level 4)*	0

where W is the weight vector of criteria and $w_i = (w_{i1}, w_{i2}, w_{i3})$ are triangular fuzzy numbers.

Step 3: The Fuzzy matrix is constructed. For m warning alternatives and n criteria for making a decision, the decision matrix can be established as:

$$D = \begin{bmatrix} \tilde{x}_{11} & \tilde{x}_{12} & \cdots & \tilde{x}_{1n} \\ \tilde{x}_{21} & \tilde{x}_{22} & \cdots & \tilde{x}_{2n} \\ \vdots & \vdots & \cdots & \vdots \\ \tilde{x}_{m1} & \tilde{x}_{m2} & & \tilde{x}_{mn} \end{bmatrix} \tag{8}$$

where $x_{ij} = (a_{ij}, b_{ij}, c_{ij})$ is triangular fuzzy number.

Step 4: The Fuzzy decision matrix was normalized. To avoid the effect of scale and unit of members in the decision matrix, the linear scale transformation was applied to transform the various criteria scales into comparable scales (Banihabib and Shabestari, 2017). The normalized fuzzy decision matrix for benefit criteria and cost criteria can be respectively represented as equations (10) and (11):

$$r_{ij} = \left[\frac{a_{ij}}{c^*_j}. \frac{b_{ij}}{c^*_j}. \frac{c_{ij}}{c^*_j} \right] \tag{9}$$

where $c^*_j = \max c_{ij}$.

$$r_{ij} = \left[\frac{\bar{a}_j}{c_{ij}}. \frac{\bar{a}_j}{b_{ij}}. \frac{\bar{a}_j}{a_{ij}} \right] \tag{10}$$

where $\bar{a}_j = \min a_{ij}$.

Step 5: Weighted normalized Fuzzy decision matrix was determined: The weighted normalized decision matrix was defined as follows:

$$v_{ij} = r_{ij}.\ w_j \tag{11}$$

where w_j represents the weight of criterion Cj.

Step 6: The Fuzzy positive ideal solution and Fuzzy negative ideal solution were calculated as follows:

$$A^* = \{v^*_1.\ v^*_2.\ \cdots.v^*_n\} \tag{12}$$

$$A^- = \{v^-_1.\ v^-_2.\ \cdots.v^-_n\} \tag{13}$$

where:

$$v^*_j = \mathrm{Max}\{v_{ij}\} i = 1.2.\ \cdots.m;\ j = 1.2.\ \cdots.n$$

$$v^-_j = \mathrm{Min}\{v_{ij}\} i = 1.2.\ \cdots.m;\ j = 1.2.\ \cdots.n$$

Since the positive triangular fuzzy numbers take the value in the interval [0, 1], $v^*_j and v^-_j$ can be defined as follows:

$v^*_j = (1.1.\ 1)$ and $v^-_j = (0.0.\ 0)$

Step 7: The distances of each alternative from fuzzy positive and negative ideal solutions were computed as:

$$s^*_i = \sum_{i=1}^{n} d(v_{ij}.\ v^*_j) i = 1.2.\ \cdots.m \tag{14}$$

$$s^-_i = \sum_{i=1}^{n} d(v_{ij}.\ v^-_j) i = 1.2.\ \cdots.m \tag{15}$$

Step 8: Closeness coefficient was calculated as:

$$CC_i = \frac{S^-_i}{S^-_i + S^*_i} i = 1.2.\ \cdots.m \tag{16}$$

Step 9: In this step, according to the values of the closeness coefficients, the flood warning alternatives can be ranked starting from the highest values and ending with the lowest value.

3. Results and discussion

3.1. Verification of the WRF model

WRF was verified based on comparison of The WRF forecasted

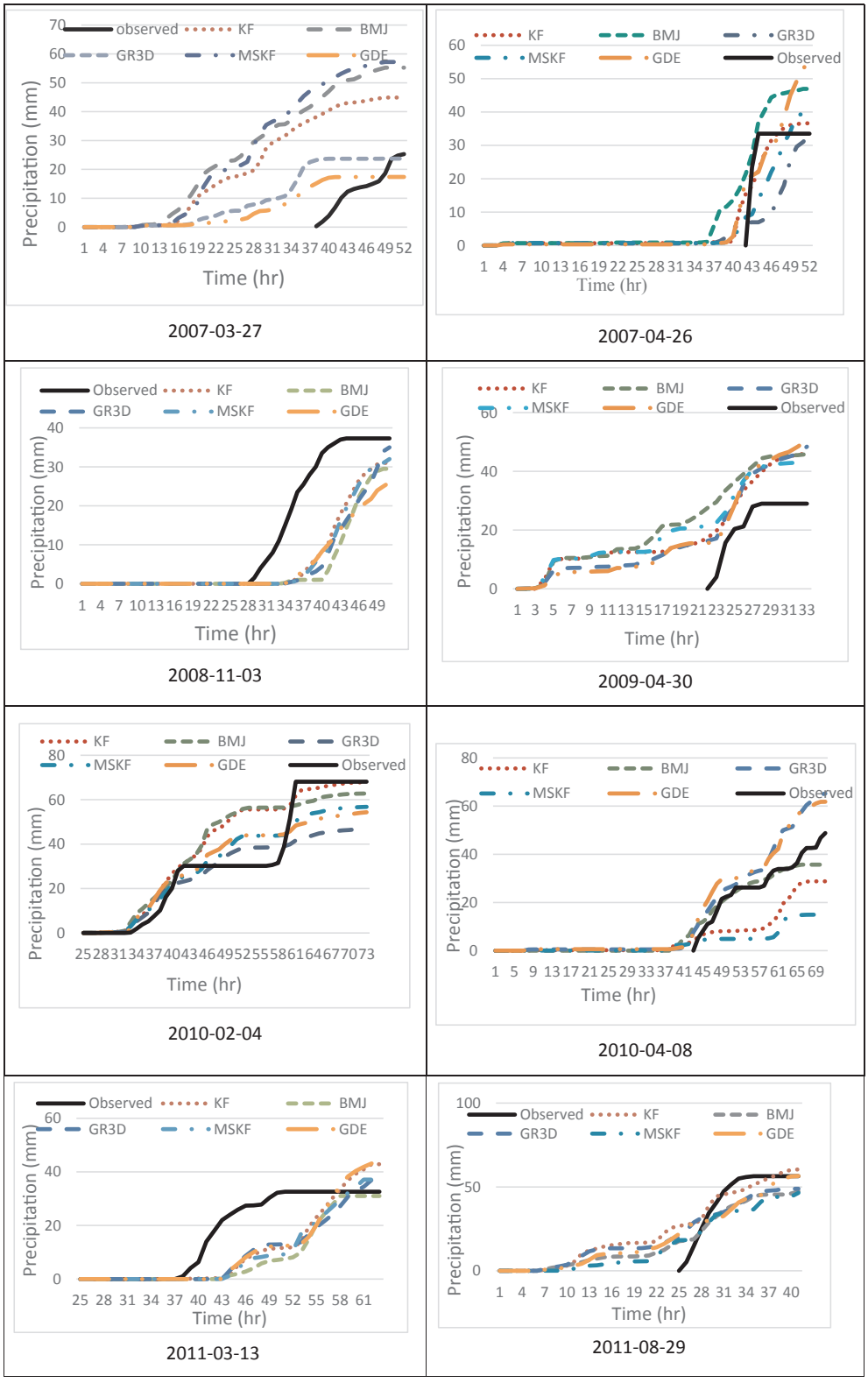

Fig. 6. The ensemble forecasted precipitation and the observed cumulative precipitation.

precipitation and gauged precipitation. The verified WRF model was applied to simulate 14 historical rainfall events. The obtained simulation results are depicted in Fig. 6. According to this Figure, the WRF model was able to capture the heavy precipitation in most events, however, the WRF model overestimates or underestimates the accumulated precipitation for some events. Since no cumulus scheme is likely to perform best for the entire events, statistical criteria are required to evaluate the overall performance. To make a further comparison, the accuracy of accumulated precipitation of the 14 flood events was computed using MARE and the results shown in Table 7. It can be seen that the WRF accumulated precipitation has a lower MARE for applying the KF scheme and a higher MARE for applying the MSKF

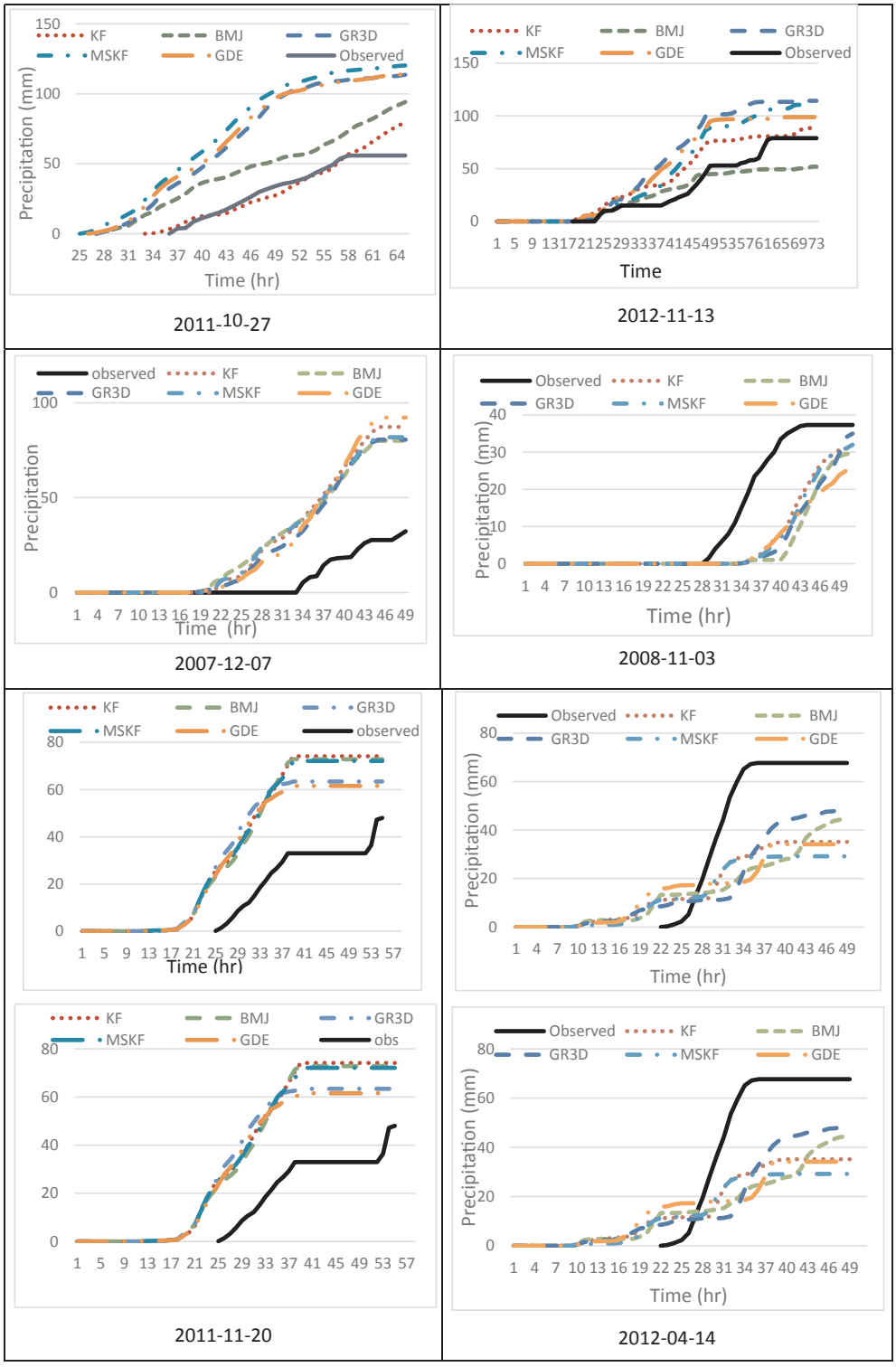

Fig. 6. (*continued*)

Table 7
MARE of the WRF model for different cumulus schemes.

Cumulus scheme	KF	BMJ	GR3D	MSKF	GDE
MARE	0.47	0.54	0.48	0.62	0.51

scheme. The KF scheme simulates convective rainfalls more accurately because the scheme conserves mass while using the parameterization of convective downdrafts as well as using convective available potential energy as part of the closure assumptions (Pennelly et al., 2014).

3.2. Verification of the Bayesian network model

In order to estimate flood peak, the WRF ensemble precipitations were fed into the Bayesian Network model. Ten different scenarios were

Table 8
Accuracy of Bayesian Network for different combinations of predictor variables of the validation set.

Combination No.	predictor variables	R^2	MARE
1	Maximum hourly rainfall	0.99	0.16
2	Accumulated rainfall	0.74	1.06
3	Maximum hourly rainfall, Base flow of the river	0.99	0.18
4	Maximum hourly rainfall, *Antecedent rainfall*	0.99	0.12
5	Maximum hourly rainfall, Base flow of the river, *Antecedent rainfall*	0.99	0.076
6	Maximum hourly rainfall (deleting KF) , Base flow of the river, Antecedent soil moisture	0.58	0.46
7	Maximum hourly rainfall (deleting BMJ) , Base flow of the river, Antecedent rainfall	0.99	0.23
8	Maximum hourly rainfall (deleting GR3D) , Base flow of the river, Antecedent rainfall	0.99	0.15
9	Maximum hourly rainfall (deleting MSKF) , Base flow of the river, Antecedent rainfall	0.99	0.087
10	Maximum hourly rainfall (deleting GDE) , Base flow of the river, Antecedent rainfall	0.99	0.10

developed using various combinations of predictors in BN. In all of the scenarios, flood peaks are the forecasted variables. The proposed Bayesian network model in the present study provides the *forecast*ed flood peaks. In a mountainous basin such as Kan basin with low floodplain storage, the peak flow magnitude is not reduced along the river, hence we can use the peak flood instead of whole flood hydrograph to estimate the flood damage.

The accuracy of the BN model for the validation data set was assessed by MARE and R^2 as shown in Table 8. The comparison between scenario No 1 and No 2 showed that the BN model driven from hourly rainfall outperformed the one using accumulated rainfall as the predictor. In small basins, such as Kan basin *with a time of concentration of 180 min*, cumulative precipitation does not represent rainfall time variation on the flood forecast and maximum hourly rainfall provides better outcomes. Therefore, the maximum hourly rainfall was used in combinations of other predictor variables in the scenarios. Moreover, comparing scenario No. 9 and 5 shows that there is no significant decrease in accuracy by deleting the MSKF scheme while deleting the KF scheme in scenario No. 6 significantly decreased the accuracy. Consequently, MSKF is the least accurate cumulus scheme and KF is the most accurate cumulus parameterization scheme in the study area. Other researches have also shown similar results on precipitation prediction (Pennelly et al., 2014; Liang et al., 2004).

According to scenario No. 5 in Table 8, the best results were achieved by applying all cumulus schemes. In this scenario, MARE was calculated 0.076 for the validation data set. The coefficient of determination, denoted by R^2, is another measure that was used to assess the accuracy of the scenarios. It can be seen from Table 8 that is also close to unity. The proposed BN structure of this scenario is composed of eight nodes as displayed in Fig. 7. The WRF ensemble precipitations, antecedent rainfall and base flow of the river are the parent nodes and peak flow magnitude is the child node. Fig. 7 also shows that base flow of the river is influenced by antecedent rainfall. Despite the small sample size of this study, the results show that the Bayesian Network is an efficient method to forecast the flood peak based on weather ensemble forecasts and it is suited for flood forecasting in case of small data set size.

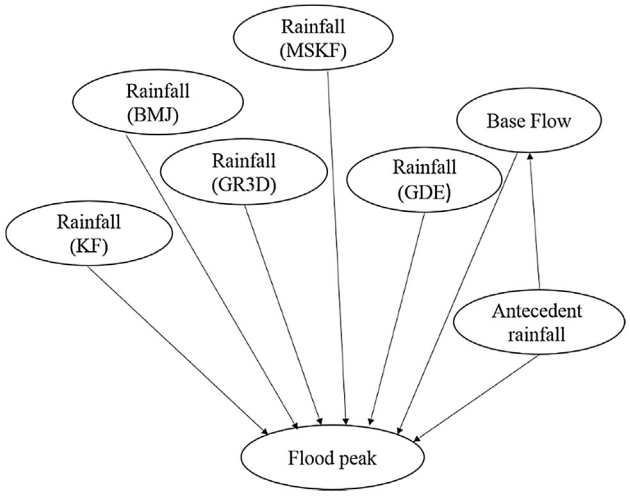

Fig. 7. The proposed structure of the Bayesian network for ensemble flood forecasting.

3.3. Effective criteria in flood warning

Due to lack of historical rainfall with high return period rainfalls during the study period, it was not possible to simulate a high variability of the return periods. Hence, the simulated floods in the present study have a return period of < 25 years with 100% probability for low warning level. Thus, some artificial storms were produced using back simulation capability of the BN model. This is explained as follows:

An example of a forecasted flood by using the BN model and its upper and lower uncertainty bands is presented in Fig. 8. As shown in Fig. 8-a, the lower and upper bounds of the uncertainty are 25.36 and 57.42 m3/s respectively. In this research, membership value of 1 was assigned to the forecasted flood peak using predicted value in scenario No. 5 (the most accurate scenario in BN) and 0 was assigned to those scenarios that forecasted the maximum and minimum flood peak among all scenarios. It can also be seen that the upper band is less than a 25-year flood, so the probability of low warning level is 100%. In order to evaluate the flood warning system for more cases, the BN backward simulation was used to produce some artificial storm events in such a way that they have different flood peaks, so the flood warning system can be evaluated on different warning levels as presented in Fig. 8-b, c, d. The backward simulation approach was used starting from the flood peak and working contrary to direction of arcs to produce the predictor nodes and then the forward simulation approached was again employed by various combinations of predictors to estimate the uncertainty bands of flood peak.

The probability of different warning levels for *forecast*ed floods was estimated by dividing the area enclosed by upper and lower bounds to the total area under the fuzzy triangle which is presented in Table 9.

The other effective criteria in flood warning decision making in flood warning system were estimated as follows:

Population at risk, flood warning costs, and flood economic damages were estimated for different warning levels as shown in Table 10. Kan River's cross sections are nearly V-shaped and there is not much difference between flood mappings for different return periods. Accordingly, there is no significant difference between populations at risk in different return periods in the studied area. This can also be found that the flood warning costs and flood economic damages have increased slightly with increasing of floods return periods. Since, according to current river regulations in Iran, the building construction in riverbed (flooded by 25-year flood) is illegal (Banihabib, 2016, Banihabib et al., 2015). The flood economic damages of unauthorized buildings in riverbed were neglected, and therefore it is calculated zero

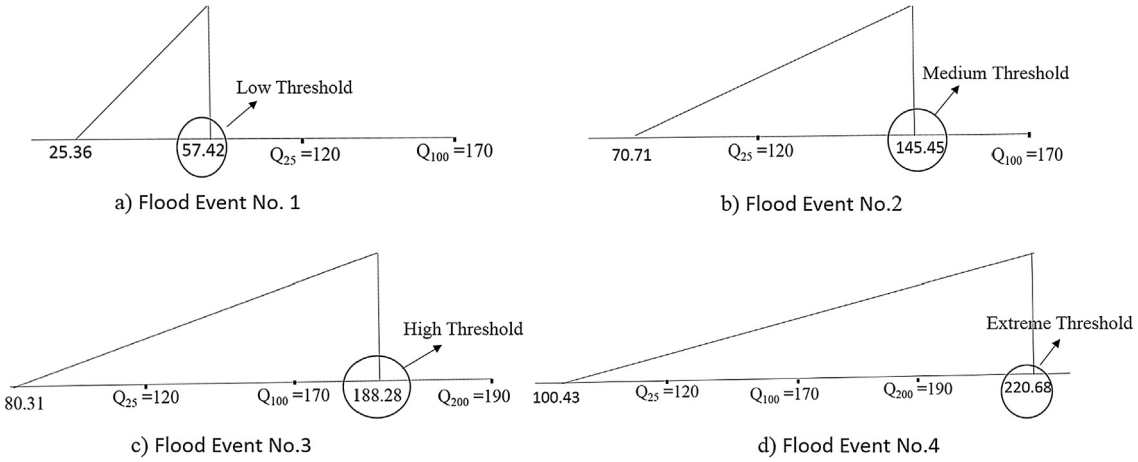

Fig. 8. The lower and upper bounds of the uncertainty of *forecast*ed flood.

Table 9
The probability of different flood warning levels in *forecast*ed floods.

Flood Event No.	Low warning	Medium warning	High warning	Extreme warning
1	100%	0	0	0
2	43%	57%	0	0
3	13%	55%	32%	0
4	3%	31%	22%	44%

for low warning level as shown in Table 10.

The expected cost of corrupted warnings and expected human losses were calculated for four forecasted flood events according to their probability of warning levels (Table 11), since these criteria are a function of the probability of different flood warning levels (as shown in Table 5 and 6). For the flood No.1, the probability of low warning level is 100%. According to the presented formulas in Table 5, the expected cost of corrupted warnings of the low warning level is a function of the probability of other flood warning levels. Since other flood warning levels have a probability of zero, this flood does not cost for the low warning level (Table 11).

There are some reasons why expected human losses listed in Table 11 may display zero. As mentioned earlier, expected human losses at each warning level is a function of the probability of three other flood warning levels. Therefore, in Table 11, the expected human losses associated with that warning level will be zero if a flood warning level has a zero probability of occurring. Besides, in cases of occurrence a warning level lower than the forecasted warning level, the residents are relocated in the safe place and human losses cannot be expected.

3.4. Weighting flood warning criteria

AHP was used to weight effective criteria using triangular fuzzy numbers as shown in Table 12. A triangular fuzzy percentage weight was assigned to each criterion between 0 and 100%, which represents the importance of the criterion as given in the last column of Table 12. A higher weight of the criterion means more priority or more impact than other criteria for warning decision. Since the probability of flood occurrence affects the other criteria (such as the expected cost of false warning and expected human losses), this criterion has the most importance and the highest weight was assigned to it.

Table 11
Expected cost of corrupted warnings (Thousand Rials) and expected human losses of missed warnings.

Flood Event No.	Warning Level	Expected cost of corrupted warnings			Expected human losses of missed warnings		
		L	M	U	L	M	U
1	Low	0	0	0	0	0	0
	Medium	549	1168	1787	0	0	0
	High	726	1543	2361	0	0	0
	Extreme	1044	2219	3394	0	0	0
2	Low	3918	7836	11,754	1.09	2.09	3.29
	Medium	132	307	455	0	0	0
	High	279	626	940	0	0	0
	Extreme	483	1088	1631	0	0	0
3	Low	6686	1337	2006	1.97	3.93	5.9
	Medium	746	1506	2257	0.29	0.59	0.88
	High	139	310	467	0	0	0
	Extreme	343	771	1158	0	0	0
4	Low	9925	19,850	29,775	3.05	6.09	9.14
	Medium	3238	6478	9717	1.18	2.35	3.53
	High	1820	3653	5481	0.57	1.13	1.70
	Extreme	170	382	544	0	0	0

*L, M, and U are respectively lower, middle and upper limit of the fuzzy triangular numbers

3.5. Decision making on warning levels

In this research, Fuzzy-TOPSIS method was employed to make a

Table 10
Population at risk, flood warning costs, and *flood economic damages* for different warning levels.

Warning Level	Population at risk			Flood warning costs (Thousand Rials)			Flood economic damages (Thousand Rials)		
	L	M	U	L	M	U	L	M	U
Low	7.6	15.2	22.8	1374	2742	4899	0	0	0
Medium	9.5	19	28.5	1522	3236	4949	705,247	840,784	1,042,889
High	10.4	20.9	31.3	1669	3547	5426	795,052	929,957	1,172,236
Extreme	11.7	23.4	35.1	1873	3981	6089	600,036	692,584	875,212

*L, M, and U are respectively lower, middle middle and upper limit of the fuzzy triangular numbers

Table 12
Fuzzy weights of different criteria in flood warning decision making.

Criteria	Weights		
	Lower	Middle	Upper
Probability of flood	0.348	0.39	0.415
Expected human losses	0.188	0.199	0.209
Economic damages	0.076	0.087	0.096
Warning costs	0.035	0.047	0.065
Expected cost of corrupted warnings	0.035	0.047	0.065
Population at risk	0.188	0.199	0.209

Table 13
The closeness coefficient and ranking of each warning level for forecasted floods.

Flood Event No.	The forecasted probability of flood warning level				Flood warning level	Closeness coefficient	Rank
	Low	Medium	High	Extreme			
1	100	0	0	0	Low	1.75	1
					Medium	1.37	4
					High	1.41	3
					Extreme	1.42	2
2	0.43	0.57	0	0	Low	1.41	4
					Medium	1.78	1
					High	1.42	3
					Extreme	1.43	2
3	0.13	0.55	0.32	0	Low	1.21	4
					Medium	1.56	2
					High	1.66	1
					Extreme	1.44	3
4	0.026	0.31	0.22	0.44	Low	1.14	4
					Medium	1.44	2
					High	1.40	3
					Extreme	1.84	1

decision on flood warning level. The closeness coefficient and the rankings of alternatives were determined for four forecasted flood events as shown in Table 13. The purpose of the present decision making is to determine the best alternative among all warning levels. The purpose of the ranking of alternatives in the present study is to find the best warning level alternative, and an order of other alternatives does not provide any decision rule for the warning.

For flood No. 1, the low warning level with the highest closeness coefficient is the best alternative. Since the probability of low warning level was estimated at 100%, it is rational to choose this warning level as the best alternative by using the decision making.

For the flood No. 2, medium warning level has the highest probability. It is clear from the results of the last two columns in Table 13 that medium warning level with the closeness coefficient of 1.78 is the best alternative as well. Since high and extreme warning levels cannot possibly happen and have a probability of zero as shown in Table 13, so selecting the medium warning level describes the rational decision.

For the flood No. 3, although the highest forecasted probability is for the medium warning level, the probability of high warning level is not zero, hence it can be seen that high warning level is in the first rank.

According to results of Table 13, it can be concluded that when the probability is distributed between different warning levels in case of a higher probability for stronger warning level (such as flood No. 2 and No. 4), the highest closeness coefficient will be achieved for the stronger warning level as the best alternative. But in case of a higher probability for milder warning level, the best alternative will generally depend on other effective criteria. In order to broaden our understanding of the decision-making behavior, there is a need for sensitivity analysis. Results of the sensitivity analysis are presented in the next section.

3.6. Sensitivity analysis on the decision making of flood warning level

Since the uncertainty was addressed in estimating the effective criteria in multi-criteria decision making, a sensitivity analysis was used only to determine how different values of probability of flood warning levels impact on decision-making behavior. The results of sensitivity analysis for different scenarios are given in Table 14. In the scenarios number 1 to 4, the probability of a specific flood warning level is 100 percent. The result shows that warning level with 100 percent probability was the selected warning level which has the highest closeness coefficient.

Scenarios number 5 to 8 were defined for a situation that the probability of one warning level is significantly higher than other warning levels. In these scenarios, an 80% probability was assigned to a warning level and the remaining 20% were assigned equally to the higher and lower warning level. It is clear from Table 14 that warning level with 80 percent probability is the selected warning level which has the highest closeness coefficient.

In scenarios number 9 to 12, a 60% probability was assigned to a warning level and the remaining 40% were assigned equally to the higher and lower warning level. The results of scenarios number 10 to 12 showed that the warning level which is most likely to occur is at the highest rank and has the highest closeness coefficient. But in scenarios number 9, although the low warning level has the highest probability of

Table 14
Sensitivity analysis of decision-making model for different scenarios.

Scenarios	The forecasted probability of flood warning level				Closeness coefficient				Ranking the warning levels			
	Low	Medium	High	Extreme	Low	Medium	High	Extreme	Low	Medium	High	Extreme
1	100%	0	0	0	1.75	1.37	1.41	1.42	1	4	3	2
2	0	100%	0	0	1.11	1.81	1.41	1.42	4	1	3	2
3	0	0	100%	0	1.11	1.17	1.84	1.42	4	3	1	2
4	0	0	0	100%	1.11	1.17	1.21	1.86	4	3	2	1
5	80%	20%	0	0	1.51	1.49	1.42	1.43	1	2	3	4
6	10%	80%	10%	0	1.16	1.58	1.48	1.44	4	1	2	3
7	0	10%	80%	10%	1.11	1.22	1.61	1.5	4	3	1	2
8	0	0	20%	80%	1.11	1.17	1.31	1.84	4	3	2	1
9	60%	40%	0	0	1.5	1.65	1.42	1.43	2	1	4	3
10	20%	60%	20%	0	1.24	1.57	1.56	1.44	4	1	2	3
11	0	20%	60%	20%	1.12	1.30	1.60	1.58	4	3	1	2
12	0	0	40%	60%	1.11	1.17	1.47	1.84	4	3	2	1
13	25%	25%	25%	25%	1.50	1.56	1.60	1.84	4	3	2	1
14	50%	50%	0	0	1.50	1.78	1.42	1.43	2	1	4	3
15	0	50%	50%	0	1.11	1.56	1.26	1.23	4	2	1	3
16	0	0	50%	50%	1.12	1.17	1.60	1.64	4	3	2	1

occurrence, the medium warning level (with 40 percent probability) is the best alternative. Therefore, it seems that when the probability is distributed between different warning levels, the decision making model acts cautiously by selecting the stronger level as the best alternative. To ensure this result, scenarios number 13 to 16 were defined so that the probability is distributed equally between two or more warning levels which in all of them the stronger warning level is the first ranked alternative as shown in Table 14. Considering all the scenarios, it could be concluded that assuming a significantly higher probability for a warning level compared to the other warning levels, the decision-making model proposes it as a warning level. However, if the probability is distributed equally between some warning levels, the decision-making model allocates a higher rank to the stronger warning level and in other words, the flood warning system acts cautiously in this case.

4. Conclusions

This study proposed a decision-making model for determining flood warning level based on atmospheric ensemble forecasts. According to knowledge of the authors, this is the first attempt to provide a flood warning system considering the ensemble forecasts and all effective criteria and uncertainty associated with them. The results showed that the WRF model was able to capture the heavy precipitation in most events, while there is an overestimation or underestimation of the accumulated precipitation in a couple of cases. While the details of the application of the WRF model are out of the purpose of the present study, possible reasons of the precipitation error were reported by other authors including; errors in the lateral boundary conditions (Ochoa et al., 2014); poor representation of the topography (Ochoa et al., 2014); and select of convective treatment, microphysics and planetary boundary layer (Jankov et al., 2005). In order to improve the forecasted rainfalls, running the WRF model using the perturbing the initial conditions and also using the different microphysical schemes are suggested as the future works.

The atmospheric ensemble forecasts were fed into the Bayesian Networks (BN) to estimate the flood peak. MARE was calculated 0.076 for validation dataset in Bayesian Network and verified that the BN is an efficient method to forecast the flood peak based on weather ensemble forecasts and it is suited for flood forecasting in case of small data set size.

Finally, the results showed that the selected warning level by the Fuzzy-TOPSIS model was strongly dependent on the probability distribution of flood warning levels and this is why the addressing of uncertainties in estimation of probability distribution is significant.

The results of the sensitivity analysis showed that in the scenarios that were given (or granted) a significantly high probability (higher than 60%) at a warning level compared to other levels, the frequent level has the highest rating. However, in the flood events where the occurrence probability was equally distributed between different warning levels, the decision-making model had assigned a higher rating to the stronger warning level. In another words, the flood warning system acts cautiously. It was also showed that Fuzzy-TOPSIS is well-suited for flood warning modeling based on ensemble forecasts. According to the reasonable results of this study, applying the proposed Fuzzy-TOPSIS model to develop a flood warning system based on atmospheric ensemble forecasts can be proposed in similar catchments for considering the uncertainties and selecting flood warning level.

Acknowledgments

The authors thank Iran's Ministry of Energy, Water, and Wastewater Standards and Projects Bureau for supporting this research through contract No. 720/1015/87.

References

Abebe, A., Price, R., 2005. Decision support system for urban flood management. J. Hydroinf. 7, 3–15.
Aguilera, P., Fernández, A., Fernández, R., Rumí, R., Salmerón, A., 2011. Bayesian networks in environmental modelling. Environ. Modell. Software 26, 1376–1388.
Banihabib, M.E., 2016. Performance of conceptual and black-box models in flood warning systems. Cogent Eng. 3, 1127798.
Banihabib, M.E., Arabi, A., Salha, A.A., 2015. A dynamic artificial neural network for assessment of land-use change impact on warning lead-time of flood. Int. J. Hydrol. Sci. Technol. 5, 163–178.
Banihabib, M.E., Shabestari, M.H., 2017. Fuzzy hybrid MCDM model for ranking the agricultural water demand management strategies in arid areas. Water Resour. Manage. 31, 495–513.
Bergmann, K., Kopp, S., 2009. GNetIc–Using bayesian decision networks for iconic gesture generation. In: International Workshop on Intelligent Virtual Agents, 2009. Springer, pp. 76–89.
Chen, F., Dudhia, J., 2001. Coupling an advanced land surface–hydrology model with the Penn State–NCAR MM5 modeling system. Part I: model implementation and sensitivity. Mon. Weather Rev. 129, 569–585.
Cloke, H., Pappenberger, F., 2009. Ensemble flood forecasting: a review. J. Hydrol. 375, 613–626.
Cooper, G.F., Herskovits, E., 1992. A Bayesian method for the induction of probabilistic networks from data. Mach. Learn. 9, 309–347.
Correa, M., Bielza, C., Pamies-Teixeira, J., 2009. Comparison of Bayesian networks and artificial neural networks for quality detection in a machining process. Expert Syst. Appl. 36, 7270–7279.
Dietrich, J., Denhard, M., Schumann, A., 2009a. Can ensemble forecasts improve the reliability of flood alerts? J. Flood Risk Manage. 2, 232–242.
Dietrich, J., Schumann, A., Redetzky, M., Walther, J., Denhard, M., Wang, Y., Pfützner, B., Büttner, U., 2009b. Assessing uncertainties in flood forecasts for decision making: prototype of an operational flood management system integrating ensemble predictions. Nat. Hazards Earth Syst. Sci. 9, 1529–1540.
Doycheva, K., Horn, G., Koch, C., Schumann, A., König, M., 2016. Assessment and weighting of meteorological ensemble forecast members based on supervised machine learning with application to runoff simulations and flood warning. Adv. Eng. Inf.
Dudhia, J., 1989. Numerical study of convection observed during the winter monsoon experiment using a mesoscale two-dimensional model. J. Atmos. Sci. 46, 3077–3107.
Grell, G.A., 1993. Prognostic evaluation of assumptions used by cumulus parameterizations. Mon. Weather Rev. 121, 764–787.
Grell, G.A., Dévényi, D., 2002. A generalized approach to parameterizing convection combining ensemble and data assimilation techniques. Geophys. Res. Lett. 29.
Guoqiang, X., Xudong, L., Hui, Y., Liping, H., Jishan, X., 2007. Precipitation simulation using different cloud-precipitation schemes for a landfall typhoon. Plateau Meteorol. 26, 891–900.
Hong, S.-Y., Dudhia, J., Chen, S.-H., 2004. A revised approach to ice microphysical processes for the bulk parameterization of clouds and precipitation. Mon. Weather Rev. 132, 103–120.
Hong, S.-Y., Noh, Y., Dudhia, J., 2006. A new vertical diffusion package with an explicit treatment of entrainment processes. Mon. Weather Rev. 134, 2318–2341.
Jankov, I., Gallus Jr., W.A., Segal, M., Shaw, B., Koch, S.E., 2005. The impact of different WRF model physical parameterizations and their interactions on warm season MCS rainfall. Weather Forecast. 20 (6), 1048–1060.
Janjić, Z.I., 1994. The step-mountain eta coordinate model: Further developments of the convection, viscous sublayer, and turbulence closure schemes. Mon. Weather Rev. 122, 927–945.
Kain, J.S., Fritsch, J.M., 1990. A one-dimensional entraining/detraining plume model and its application in convective parameterization. J. Atmos. Sci. 47, 2784–2802.
Klein, C., Heinzeller, D., Bliefernicht, J., Kunstmann, H., 2015. Variability of West African monsoon patterns generated by a WRF multi-physics ensemble. Clim. Dyn. 45, 2733–2755.
Komma, J., Reszler, C., Blöschl, G., Haiden, T., 2007. Ensemble prediction of floods? catchment non-linearity and forecast probabilities. Nat. Hazards Earth Syst. Sci. 7, 431–444.
Li, J., Chen, Y., Wang, H., Qin, J., Li, J., Chiao, S., 2017. Extending flood forecasting lead time in a large watershed by coupling WRF QPF with a distributed hydrological model. Hydrol. Earth Syst. Sci. 21, 1279.
Liang, X.Z., Li, L., Dai, A., Kunkel, K.E., 2004. Regional climate model simulation of summer precipitation diurnal cycle over the United States. Geophys. Res. Lett. 31.
Madigan, D., York, J., Allard, D., 1995. Bayesian graphical models for discrete data. Int. Stat. Rev./Revue Internationale de Statistique 215–232.
Mlawer, E.J., Taubman, S.J., Brown, P.D., Iacono, M.J., Clough, S.A., 1997. Radiative transfer for inhomogeneous atmospheres: RRTM, a validated correlated-k model for the longwave. J. Geophys. Res. Atmos. 102, 16663–16682.
Nasrollahi, N., Aghakouchak, A., Li, J., Gao, X., Hsu, K., Sorooshian, S., 2012. Assessing the impacts of different WRF precipitation physics in hurricane simulations. Weather Forecasting 27, 1003–1016.
Ochoa, A., Pineda, L., Crespo, P., Willems, P., 2014. Evaluation of TRMM 3B42 precipitation estimates and WRF retrospective precipitation simulation over the Pacific-Andean region of Ecuador and Peru. Hydrol. Earth Syst. Sci. 18, 3179–3193.
Pennelly, C., Reuter, G., Flesch, T., 2014. Verification of the WRF model for simulating heavy precipitation in Alberta. Atmos. Res. 135, 172–192.
Raftery, A.E., Gneiting, T., Balabdaoui, F., Polakowski, M., 2005. Using Bayesian model averaging to calibrate forecast ensembles. Mon. Weather Rev. 133, 1155–1174.

Reed, E., Mengshoel, O.J., 2014. Bayesian network parameter learning using EM with parameter sharing. In: Proceedings of the Eleventh UAI Conference on Bayesian Modeling Applications Workshop-Volume 1218. Citeseer, pp. 48–59.
Rogelis, M.C., Werner, M. Streamflow forecasts from WRF precipitation for flood early warning in mountain tropical areas.
Saaty, R.W., 1987. The analytic hierarchy process—what it is and how it is used. Math. Modelling 9, 161–176.
Sharma, A., Goyal, M.K., 2016. Bayesian network for monthly rainfall forecast: a comparison of K2 and MCMC algorithm. Int. J. Comput. Appl. 38, 199–206.
Shrivastava, R., Dash, S., Oza, R., Sharma, D., 2014. Evaluation of parameterization schemes in the WRF model for estimation of mixing height. Int. J. Atmos. Sci.(2014).
Sikder, S., Hossain, F., 2016. Assessment of the weather research and forecasting model generalized parameterization schemes for advancement of precipitation forecasting in monsoon-driven river basins. J. Adv. Model. Earth Syst. 8, 1210–1228.
Tian, J., Liu, J., Wang, J., Li, C., Yu, F., Chu, Z., 2017. A spatio-temporal evaluation of the WRF physical parameterisations for numerical rainfall simulation in semi-humid and semi-arid catchments of Northern China. Atmos. Res. 191, 141–155.
Wang, T.-C., Chang, T.-H., 2007. Application of TOPSIS in evaluating initial training aircraft under a fuzzy environment. Expert Syst. Appl. 33, 870–880.
Yang, B., Qian, Y., Lin, G., Leung, R., Zhang, Y., 2012. Some issues in uncertainty quantification and parameter tuning: a case study of convective parameterization scheme in the WRF regional climate model. Atmos. Chem. Phys. 12, 2409.
Yang, T.-H., Gong-Do, H., Chin-Cheng, T., Jui-Yi, H., 2016. Using rainfall thresholds and ensemble precipitation forecasts to issue and improve urban inundation alerts. Hydrol. Earth Syst. Sci. 20, 4731.
Zhang, R., Bivens, A.J., 2007. Comparing the use of bayesian networks and neural networks in response time modeling for service-oriented systems. In: Proceedings of the 2007 workshop on Service-oriented computing performance: aspects, issues, and approaches, 2007. ACM, pp. 67–74.
Zheng, Y., Alapaty, K., Herwehe, J.A., del Genio, A.D., Niyogi, D., 2016. Improving high-resolution weather forecasts using the Weather Research and Forecasting (WRF) Model with an updated Kain-Fritsch scheme. Mon. Weather Rev. 144, 833–860.